Propagating the uncertainties of the overhead line span vulnerability model up to the failure return period in case of extreme events

Elisa Ferrario
Energy System Development Dept.
Ricerca sul Sistema Energetico S.p.A.
Milan, Italy
elisa.ferrario@rse-web.it

Andrea Pitto
Energy System Development Dept.
Ricerca sul Sistema Energetico S.p.A.
Milan, Italy
andrea.pitto@rse-web.it

Emanuele Ciapessoni
Energy System Development Dept.
Ricerca sul Sistema Energetico S.p.A.
Milan, Italy
emanuele.ciapessoni@rse-web.it

Diego Cirio
Energy System Development Dept.
Ricerca sul Sistema Energetico S.p.A.
Milan, Italy
diego.cirio@rse-web.it

2024 3rd International Conference on Energy Transition in the Mediterranean Area (SyNERGY MED) | 979-8-3503-7592-3/24/$31.00 ©2024 IEEE | DOI: 10.1109/SyNERGYMED62435.2024.10799235

***Abstract*—The operation of electric power systems may be affected by the failure of system components due to adverse weather events. Consequently, the assessment of the "resilience" property, meant as the ability to limit the extent, severity, and duration of system degradation due to such disruptive events, becomes a fundamental task. In resilience analyses, uncertainty sources should be properly represented and quantified. This work proposes an approach based on the Point Estimation Method (PEM) to assess the probability distributions of the failure return periods of overhead line spans, starting from the uncertainties in the span vulnerability model. The approach is applied to three transmission lines exposed to wind loads. Results show that PEM is suitable for uncertainty propagation in the resilience assessment methodology. In particular, different behaviors of the spans are highlighted, in terms of uncertainty of their failure probabilities.**

Keywords—electric power system, vulnerability, resilience, uncertainty propagation, Point Estimation Method.

I. INTRODUCTION

Electric power systems are exposed to many threats, such as extreme weather events, that may damage some of their components compromising their proper functioning. In this context, "resilience" property, defined by CIGRE as "the ability to limit the extent, severity, and duration of system degradation following an extreme event" [1][2], has become of paramount importance.

Resilience analysis of an electric power system considers the frequency and severity of a hazard, e.g. a weather event, and the vulnerability of the grid components and assets. The resilience assessment methodology in [3] and [4] has been developed to include these aspects and to support the transmission grid planning by calculating resilience indicators and quantifying the benefit that can be achieved with appropriate interventions on the grid, accounting for multiple contingencies and potential cascading outages. However, every step of the methodology is affected by uncertainties in the input variables and parameters of the mathematical models, which makes it important to analyze the propagation of these uncertainties on the outcomes.

In the scientific literature, uncertainty in risk and resilience analyses is distinguished into two types: aleatory uncertainty (also referred to objective, stochastic and irreducible uncertainty) due to the inherent variability in the system behavior, and epistemic uncertainty (also referred to subjective and reducible uncertainty) due to lack of knowledge and information on the system [5][6]. Depending on the types of uncertainty and on the available information, different approaches, e.g. pure probabilistic, non-probabilistic and hybrid approaches, can be used to represent, propagate, and quantify uncertainty through a mathematical model.

Pure probabilistic approaches represent both the aleatory and epistemic uncertainties by means of probability distributions [7][8]. Non-probabilistic approaches provide an alternative representation of the epistemic uncertainty by using possibility distributions, intervals and fuzzy logic to account for the lack of data and information that may prevent the construction of probability distributions with an acceptable statistical accuracy [9][10]. Hybrid approaches combine pure probabilistic and non-probabilistic approaches to properly represent both aleatory and epistemic variables [7][8][10]. Other methods to quantify uncertainty in the context of electric power systems have also been adopted in the scientific literature, such as Information Gap Decision Theory, Robust Optimization, and Distributionally Robust Optimization [11][12][13].

This work focuses on probabilistic approaches and specifically on the Point Estimation Method (PEM) [14][15], that provides the statistical moments of the output variables by carrying out a limited number of evaluations, e.g. only two samples for each input parameter. The PEM-based proposed approach is exploited in order to propagate the uncertainty of one input parameter of the span vulnerability model, i.e. the span initial mechanical tension, to one outcome, i.e. the span failure return period. The method is applied to three transmission lines, and the first four statistical moments of the failure return periods of each span are estimated. Then, the related probability distributions are obtained.

The sequel of the paper is organized as follows. In Section II, the mathematical background related to the resilience assessment framework is shortly recalled; Section III describes the proposed uncertainty propagation methodology; the case study and the relevant results are discussed in Section IV; Section V provides some conclusions. Finally, Appendix briefly recalls the PEM and the Gram-Charlier expansion.

979-8-3503-7592-3/24/$31.00 ©2024 IEEE

II. VULNERABILITY MODELING IN THE RESILIENCE ASSESSMENT FRAMEWORK: A RECALL

The methodology for long term resilience assessment in [4] is able to compute the return periods for substation outages and the expected energy not supplied in the Italian electric power transmission grid after the occurrence of disruptive weather events. An intermediate result to achieve the indicators above consists of the failure return periods for grid components, especially overhead transmission lines, which are the most susceptible components to wind and snow threats.

The three main steps for the computation of the transmission line span failure return periods are briefly recalled in the following, whereas the complete methodology is fully described in [3][4].

The first step is related to the probability of occurrence of a weather event, that is typically represented using a complementary cumulative distribution function (CCDF), whose associated probability density function (PDF) is denoted, in the rest of the paper, as $f_{C(l,t)}(th)$ with respect to a generic transmission line span l, a climatological period t, and a specific value, th, of the stress variable associated with the threat under study.

The second step computes the vulnerability curves of each single subcomponent of the transmission line span l, such as conductors, towers, shield wires, and foundations. The vulnerability curves are built on the basis of specific technical and orographic parameters and represent the failure probability of the subcomponents given a severity level of the stress variables under analysis, e.g. the stress variable associated with the weather event threshold, as described by the authors in [16]. The vulnerability model of each subcomponent is given by a lognormal function centered on the expected value of the mechanical component resistance. Then, from the failure probability of each subcomponent, the vulnerability of the transmission line span l, $P_{V_l}(th)$, associated with the weather event threshold, th, is calculated by considering all subcomponents in series.

Finally, the third step regards the computation of the failure probability, $P_{F(l,t)}$, of the transmission line span l, with respect to the climatological period t, that is given by the integral of the product between the vulnerability model of the line span l, P_{V_l}, and the PDF of the weather event, $f_{C(l,t)}$, as illustrated in (1). The corresponding failure return period, $RP_{F(l,t)}$, is computed as the inverse of the failure probability, $P_{F(l,t)}$, as reported in (2).

$$P_{F(l,t)} = \int P_{V_l}(th)\, f_{C(l,t)}(th) dth \quad (1)$$

$$RP_{F(l,t)} = 1/P_{F(l,t)} \quad (2)$$

III. UNCERTAINTY PROPAGATION METHOD

This Section describes the proposed approach based on PEM for the propagation of the uncertainties related to the asset vulnerability model.

A. Vulnerability model and failure return period in presence of uncertainty

Let us define as p_l an uncertain aleatory input parameter of span l, such as the span initial mechanical tension, that enters the vulnerability model, P_{V_l}, and as f_{p_l} its PDF. In presence of uncertainty, the vulnerability model of span l exposed to the occurrence of a weather event with threshold th is updated, as illustrated in (3):

$$P_{V_l}^{new}(th) = \int P_{V_l}(th, p_l)\, f_{p_l}(p_l) dp_l \quad (3)$$

Then, the new vulnerability model, $P_{V_l}^{new}$, is adopted to compute the failure return period, $RP_{F(l,t)}^{new}$, of line span l for the climatological period t, as in (4):

$$RP_{F(l,t)}^{new} = 1/\int P_{V_l}^{new}(th)\, f_{C(l,t)}(th) dth \quad (4)$$

B. Main steps of the uncertainty propagation method

The proposed uncertainty propagation approach uses the PEM integrated within the resilience assessment methodology in order to propagate the uncertainty of one input parameter of the span vulnerability model, specifically, the span initial mechanical tension, to one outcome of the methodology, i.e. the span failure return period, with respect to a weather threat of interest. It is worth noting that the approach is general and can be applied to both wind and snow threats, which are the threats causing the largest contribution to energy not served in the Italian transmission system. This paper focuses on its application to the wind threat.

A short description of PEM is provided in the Appendix, whereas the main steps for uncertainty propagation are given below:

1. Define vector $\bar{\alpha}=\{\alpha_1, \alpha_2, \ldots, \alpha_r, \ldots, \alpha_R\}$ of R threshold values associated with the weather threat; for example, for the wind threat, vector $\bar{\alpha}$ contains wind speed values, e.g. $\bar{\alpha}=\{100,120,\ldots,200\}$ [km/h].
2. Define vector $\bar{\mu}_p = \{\mu_{p_1}, \mu_{p_2}, \ldots, \mu_{p_l}, \ldots, \mu_{p_m}\}$ of the expected values of the uncertain parameter p_l for each span l, l=1,…,m, where m is the number of spans of a transmission line.
3. Represent the parameter p_l by means of a PDF, f_{p_l}, given by a uniform distribution, assuming the domain of existence of the PDF between two extreme values given by $\mu_{p_l} \pm q\mu_{p_l}$, where q represents a percentage of the expected value.
4. Compute the PEM parameter location $p_{l,k}$ and the PEM weight $w_{l,k}$ for each span l, l=1,…,m, and k=1, 2 ,3, by using (A.1)-(A.3) (see Appendix). At the end of this steps, a matrix of dimension $m \times k$ is obtained both for the parameter locations and the weights.
5. For each threshold α_r, r=1,…,R, for each k, k=1,2,3, and for each span l, l=1,…,m, run m times (for s, s=1,…,m) the vulnerability model by using as input vector $\bar{\mu}_p$ (defined in step 2 above), and by replacing each time for span s, s=1,…,m, the expected value, μ_{p_l}, with the parameter location $p_{l,k}$, when l=s, and keeping the expected values μ_{p_l} for the other spans when $l \neq s$, as required by PEM (see Appendix). At the end of this step, $3m$ vulnerability curves are obtained for each span l. Since the last m vulnerability curves, those for k=3, are all the same, only $2m$+1 vulnerability curves are considered in the following. Fig. 1 represents a sketch of the obtained vulnerability curves in the form of numerical matrices for a generic span.
6. Combine the vulnerability curve, $P_{V_{l,s,k}}^{new}$, and the weather function, $f_{C(l,t)}$, to obtain the return period, $RP_{F(l,s,k,t)}^{new}$, l=1,…,m, s=1,…,m, k=1, 2, 3 for the climatological period t. More in detail, compute the

inverse of the integral of the product of the vulnerability curve and the weather curve, as in (4).

7. For each span s=1,…,m, obtain the first four central moments, $\theta_{s,j}$, j=1, 2, 3, 4 of the return periods $RP^{new}_{F(l,s,k,t)}$ by using (A.4) and (A.5) and apply Gram-Charlier (GC) series expansion (A.6) to estimate the corresponding PDF. GC series expansion provides good convergence properties for the typical ranges of parameters used in common engineering applications. Notice that the applied methodology has no limitation with respect to the shape of the generated PDFs.

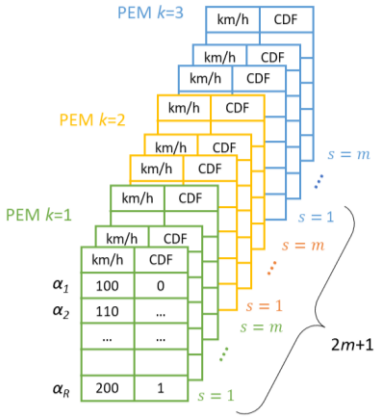

Fig. 1. Vulnerability matrices related to the wind threat obtained at the end of step 5 of the algorithm for uncertainty propagation, for a generic span and for the 2m+1 different PEM evaluations. The evaluations of PEM for k=3 are all the same.

IV. Case Study

A. Description

Three High Voltage (HV) transmission lines, whose parameters are within the range of real HV lines, are considered. Line 1, Line 2, and Line 3 are composed by 79, 51 and 14 spans, respectively, with different lengths. For illustration purposes, Fig. 2 shows a simplified representation of Line 3, indicating the 14 spans, the type of connections between the spans, tension clamps or suspension clamps, and the corresponding sections. A line section refers to a group of consecutive spans connected by suspension clamps and included within two consecutive tension clamps, and a line is the group of all the associated spans. Both tension clamps and suspension clamps are designed to support conductors in correspondence with towers, but tension clamps keep the insulator chains more stable avoiding their movements, while suspension clamps allow limited movements to insulator chains.

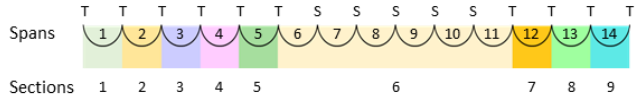

Fig. 2. Illustration of the 14 line spans of Line 3, the types of connections (T = tension clamps and S = suspension clamps), and the line sections.

As mentioned in Section III.B, the initial mechanical tension, expressed in N, of the conductor of a transmission line span is taken as the uncertain input parameter and it is represented in probabilistic terms by using a uniform PDF. This parameter depends on the line design and installation and can impact the span sag, the probability of flashover, the tensions applied to subcomponents (towers, cross-arms, conductors, shield wires) at a specific level of threat (e.g. specific wind loads): the higher the initial mechanical tension, the higher the tension in presence of loads (such as wind loads). Then, also the span failure probability that depends on all the mentioned elements is affected by the initial tension. A sensitivity analysis is carried out with respect to the domain of the uniform PDF, by selecting three different values of the parameter q, i.e. q=0.05, 0.10, 0.20 (step 3 of Section III.B).

B. Effects of the uncertainty level on vulnerability models

PEM is applied within the resilience assessment methodology to propagate the uncertainty of the span initial mechanical tension, entering the vulnerability model, to the span failure return period.

In Fig. 3 the vulnerability functions of span l=6 of Line 3, obtained for different PEM evaluation, k=1, 2, 3, of the initial mechanical tension, are reported for different values of the parameter q, q=0.05, 0.10, 0.20.

A slight difference of the vulnerability can be noticed around 150 km/h of wind speed; as expected, the higher the q values, the higher the upper and lower bounds of the function, given by k=1 and k=2, respectively. Also, span l=6 has vulnerability equal to zero below 140 km/h, which means that its probability of failure is not negligible only for higher values of wind speed. These results are obtained at the end of step 5 of the procedure illustrated in Section III.B.

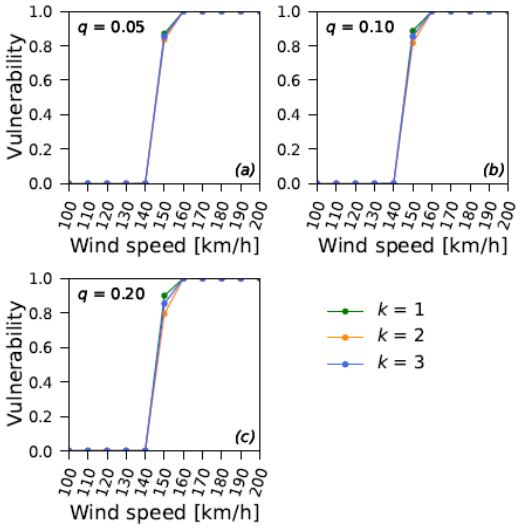

Fig. 3. Vulnerability functions of span l=6 of Line 3, obtained for different PEM evaluation, k=1, 2, 3, of the initial tension and for different values of the parameter q, q=0.05, 0.10, 0.20, in (*a*), (*b*), and (*c*), respectively.

C. Quantification of the uncertainty on failure return periods for line spans

The vulnerability CDFs of the previous Section IV.B. are combined with the PDF of the weather events based on wind speed to compute the failure return period of each span, $RP^{new}_{F(l,s,k,t)}$, l=1,…,m, s=1,…,m, k=1, 2, 3 for the climatological period t, as described in step 6 of the methodology of Section III.B. It is worth mentioning that the probability of having an event with wind speed higher than 140 km/h is very low, e.g. it is equal to 0.015 for span l=6. Thus, in order to analyze a more critical case, in this work, the climate PDF is shifted on the right by 50 km/h. After the shift, for example, the probability of having an event of wind speed higher than 140 km/h for span l=6 is increased up to 0.148. Table I provides the mean (raw moment of order 1, $\vartheta_{l,1}$), the variance (central moment of order 2, $\theta_{l,2}$) and the skewness and the kurtosis (i.e. the standardized central moments $\hat{\theta}_{l,3}$ and $\hat{\theta}_{l,4}$, respectively)

of the failure return period of four spans, l=2, 6, 8 and 10 for different values of the parameter q, q=0.05, 0.10, 0.20. Fig. 4 shows the corresponding PDFs for span l=6 obtained by applying Gram-Charlier expansion. Since these PDFs are obtained by a series expansion, it may occur that few PDF values go slightly below zero. From Fig. 4, it can be noticed that, as expected, the higher the q value, the larger is the standard deviation of the PDFs, corresponding to a higher value of the second central moments ($\theta_{l,2}$, in Table I). Span l=2 has the largest standard deviation of return periods, approximately 0.45 years for q=0.20; instead, spans l=6, 8, 10 present approximately a standard deviation of failure return periods of less than 0.17 years for q=0.20. Also, the peaks of the PDFs move to slightly higher return periods by increasing the parameter q. The PDFs are not symmetric, e.g. for q=0.20, the skewness ($\hat{\theta}_{l,3}$) is equal to 0.69 for span l=2, and 0.26 for l=6. Finally, the kurtosis, $\hat{\theta}_{l,4}$, in Table I, shows similar values lower than 3, the reference value for normal distribution.

In Table I the coefficient of variation (COV) of the failure return period, given by the percentage ratio between the standard deviation (square root of the central moment of order 2) and the mean (raw moment of order 1, $\vartheta_{l,1}$), is also reported. As expected, the higher q, the higher the COV. The highest value of COV is equal to 0.85% and occurs for span l=2, previously identified as the one with largest uncertainty.

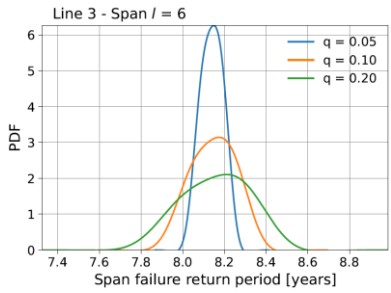

Fig. 4. PDFs of the failure return periods of spans l=6 of Line 3 for different values of the parameter q.

Results related to Line 1 and Line 2 are not reported here for brevity. Similar considerations can be carried out for most of their spans, i.e. the uncertainty in the return periods due to initial mechanical tension uncertainties is quite limited. However, there are also few exceptions, i.e. spans that have a return period characterized by larger uncertainty. For illustration purposes, Fig. 5 shows the PDF of span 41 of Line 2 obtained by applying Gram-Charlier expansion for different values of the parameter q, q=0.05, 0.10, 0.20. The return period of this span is characterized by larger uncertainty, e.g. the associated COV is equal to 3.88 %, 6.92% and 10.19% for q=0.05, 0.10 and 0.20, respectively.

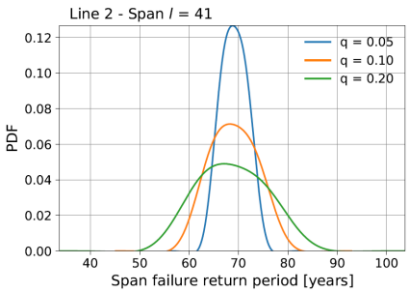

Fig. 5. PDFs of the failure return periods of spans l=41 of Line 2 for different values of the parameter q.

V. Conclusions

An innovative uncertainty propagation approach based on PEM has been proposed and applied to a methodology for resilience analysis of electric power systems in order to propagate the uncertainty associated with the span initial mechanical tension inside the vulnerability model to the span failure return period, which is an intermediate outcome of the methodology. Uncertainty has been modeled in probabilistic terms by using a uniform distribution function for the uncertain parameter and a sensitivity analysis on its domain has also been carried out.

The methodology has been applied to three HV transmission line spans exposed to strong wind threat; the proposed approach is general and can be applied to, e.g, both wind and wet snow threats. The validation of results would be of interest, but currently there are no historical data showing the dependence of the energy not supplied on the uncertainty of the initial mechanical tension. However, the results show that PEM is effective in propagating the uncertainty of the initial mechanical failure, by providing a PDF of the failure return period for each span and for each level of uncertainty. Results also reveal a variety of behaviors of the line spans in terms of uncertainty of their failure return periods, even though for all spans of Line 3 and for most of the spans of Line 1 and Line 2 the uncertainty in the failure return periods is quite limited. Moreover, the PDFs of the failure return periods are generally characterized by a not null (prevalently positive) skewness. Further work will consist in applying approaches similar to the one here proposed, in order to analyze other factors (e.g. different threats) that affect the resilience analysis.

Acknowledgment

This work has been financed by the Research Fund for the Italian Electrical System under the Three-Year Research Plan 2022-2024 (DM MITE n. 337, 15.09.2022), in compliance with the Decree of April 16th, 2018.

Table I. Mean ($\vartheta_{l,1}$), variance ($\theta_{l,2}$) and skewness ($\hat{\theta}_{l,3}$) and kurtosis ($\hat{\theta}_{l,4}$) of the return periods of spans l=2, 6, 8 and 10 of Line 3 for different values of the parameter, q=0.05, 0.10, 0.20, and corresponding coefficient of variation (COV) [%].

q	Span l	*Mean* ($\vartheta_{l,1}$)	*Variance* ($\theta_{l,2}$)	*Skewness* ($\hat{\theta}_{l,3}$)	*Kurtosis* ($\hat{\theta}_{l,4}$)	*COV [%]*
0.05	2	7.680334	0.004272	0.336888	1.819098	0.85
	6	8.139473	0.002963	0.095988	1.801515	0.67
	8	9.312164	0.002502	0.972178	1.975383	0.54
	10	9.080891	0.001339	-0.992202	1.984575	0.40
0.10	2	7.699756	0.021073	0.459345	1.835765	1.89
	6	8.145458	0.012008	0.177975	1.805290	1.35
	8	9.315207	0.003018	0.975523	1.976864	0.59
	10	9.105711	0.004128	0.085523	1.801222	0.71
0.20	2	7.813837	0.200198	0.698520	1.884880	5.73
	6	8.155454	0.027504	0.260082	1.811332	2.03
	8	9.318892	0.018132	0.562952	1.845589	1.44
	10	9.110274	0.016700	0.221415	1.806698	1.42

REFERENCES

[1] E. Ciapessoni, D. Cirio, A. Pitto, M. Panteli, M. Van Harte, C. Mak, "Defining power system resilience," ELECTRA, vol. 306, pp. 1-3, 2019.

[2] E. Ciapessoni, D. Cirio, A. Pitto, M. Van Harte and M. Panteli, "Power System Resilience: definition, features and properties," CIGRE Science and Engineering J., vol. 30, pp. 1-40, Oct. 2023.

[3] TERNA and RSE, "Addendum A.76 of the Grid Code," 2022. [Online]. Available: https://download.terna.it/terna/Allegato%20A76_Metodologia%20per%20il%20calcolo%20dell%E2%80%99incremento%20della%20resilienza%20della%20RTN_8da0cb083714ad4.pdf.

[4] E. Ciapessoni, A. Pitto, D. Cirio, E.M. Carlini, F. Marzullo, S. Casulli, F. Falorni, et al., "Application of a multi-hazard risk-based Resilience assessment methodology to real cases in the Italian Transmission System," 2024 CIGRE General Session, Paris, Aug 25-30, 2024.

[5] G. E. Apostolakis, "The concept of probability in safety assessment of technological systems," Science, vol. 250, n. 4986, pp. 1359-64, 1990.

[6] J.C. Helton, J.D. Johnson, W.L. Oberkampf, "An exploration of alternative approaches to the representation of uncertainty in model predictions," Reliab. Eng. Syst. Saf., vol. 85(1-3), pp. 39-71, 2004.

[7] E. Zio and N. Pedroni, "Literature review of methods for representing uncertainty," N° 2013-03 of the Industrial safety reports, Foundation for an Industrial Safety Culture, ISSN 2100-3874, France, 2013.

[8] M. Salimi, M. -A. Nasr, S. H. Hosseinian, G. B. Gharehpetian e M. Shahidehpour, "Information gap decision theory-based active distribution system planning for resilience enhancement," IEEE Transactions on Smart Grid, vol. 11, n. 5, pp. 4390 - 4402, 2020.

[9] D. Dubois, "Possibility theory and statistical reasoning," Computational Statistics & Data Analysis, vol. 51, n. 1, 2006.

[10] S. Ferson, D. R. J. Moore, P. J. Van den Brink, T. L. Estes, K. Gallagher, R. O'Connor and F. Verdonck., Chapter "Bounding uncertainty analyses", CRC Press, pp. 89–122, 2010.

[11] A. Soroudi and T. Amraee, "Decision making under uncertainty in energy systems: State of the art," Renewable and Sustainable Energy Reviews, vol. 28, pp. 376-384, 2013.

[12] G. Chicco, "Data consistency for data-driven smart energy assessment," Frontiers in Big Data, vol. 4, pp 1-19, 2021.

[13] V. Singh, T. Moger and D. Jena, "Uncertainty handling techniques in power systems: A critical review," Electric Power Syst. Res., vol. 203, pp. 1-20, 2022.

[14] J. M. Morales and J. Pérez-Ruiz, "Point Estimate Schemes to Solve the Probabilistic Power Flow," IEEE Trans. Power Syst., vol. 22, n. 4, pp. 1594–1601, 2007.

[15] E. Rosenblueth, "Point estimates for probability moments," Proc. Nat. Acad. Sci., vol. 72, n. 10, pp. 3812–3814, 1975.

[16] E. Ciapessoni et al., "Modeling the overhead line vulnerability to combined wind and snow loads for resilience assessment studies," 2021 IEEE Madrid PowerTech, Madrid, Spain, pp. 1-6, 2021.

[17] E. Jondeau and M. Rockinger, "Gram–Charlier densities," Journal of Economic Dynamics and Control, vol. 25, n. 10, pp. 1457-1483, 2001.

APPENDIX

A. Point Estimation Method

The Point Estimation Method (PEM) [14][15] is a technique aimed at computing the moments of a random variable Z that is a function of m random input variables p_l, $Z=F(p_1, p_2, \ldots, p_l, \ldots, p_m)$, which are uncertain and represented in probabilistic terms by a PDF, f_{p_l}, with mean μ_{p_l} and standard deviation σ_{p_l}. PEM estimates the output Z considering few points, e.g. 3 referred to the index location k, k=1, 2, 3, for each variable, p_l, l=1,...,m, where each point is defined by a pair composed by a location, $p_{l,k}$, and a weight $w_{l,k}$, l=1,..,m, k=1, 2, 3. The location represents the value at which the function F is evaluated and the weight defines the relative importance of this evaluation with respect to the output Z, see (A.1)-(A.3) below.

Different PEM schemes are available. The present work adopts the $2m$+1 scheme, which provides a suitable tradeoff between accuracy and computational burden. This means that for m stochastic variables, p_l, l = 1,...,m, the method requires the evaluation of Z over $2m$+1 different points, leading to outputs $Z_{l,k}$, l = 1,..,m, k = 1, 2, 3. The $2m$+1 different points are selected as follows:

- For locations k=1 or k=2, m vectors are built, one vector for each stochastic variables, p_l, where at each evaluation l, l=1,...,m, the input vector to the function F is given by the location $p_{l,k}$ and by the mean values of the m-1 remaining inputs. For example, the first evaluation (l=1) is $Z_{1,k} = F(p_{1,k}, \mu_{p_2}, \ldots, \mu_{p_m})$.
- For location k=3, the mean values for all stochastic inputs are used, e.g. $Z_{1,3} = F(\mu_{p_1}, \mu_{p_2}, \ldots, \mu_{p_l}, \ldots, \mu_{p_m})$, $Z_{2,3} = F(\mu_{p_1}, \mu_{p_2}, \ldots, \mu_{p_l}, \ldots, \mu_{p_m})$, etc. Notice that also for k=3, m vectors can be built, but one evaluation is sufficient because by replacing the mean value each time, m identical PEM evaluations are obtained; for this reason, the adopted PEM scheme is called "2m+1".

The k-th location $p_{l,k}$ of variable p_l, l = 1,...,m, is evaluated according to (A.1):

$$p_{l,k} = \mu_{p_l} + \xi_{l,k}\sigma_{p_l} \tag{A.1}$$

where $\xi_{l,k}$ is the standard location given by (A.2) for k=1, 2, 3:

$$\xi_{l,k} = \frac{\lambda_{l,3}}{2} + (-1)^{3-k}\sqrt{\lambda_{l,4} - \frac{3\lambda_{l,3}^2}{4}}, k = 1,2 \qquad \xi_{l,3} = 0 \tag{A.2}$$

where $\lambda_{l,3}$ and $\lambda_{l,4}$ are the third and fourth standard central moments of the variable p_l.

The k-th weight $w_{l,k}$ of variable p_l, l = 1,..,m, is evaluated according to (A.3) for k = 1, 2, 3.

$$w_{l,k} = \frac{(-1)^{3-k}}{\xi_{l,k}\cdot(\xi_{l,1}-\xi_{l,2})},\ k = 1,2 \qquad w_{l,3} = \frac{1}{m} - \frac{1}{\lambda_{l,4}-\lambda_{l,3}^2} \tag{A.3}$$

After estimating all outputs $Z_{l,k}$, l=1,..,m, k=1, 2, 3, the first raw moments, ϑ_j, e.g. j=1, …, 4 , of output Z are obtained by (A.4), where E stands for the "expectation value" operator.

$$\vartheta_j = E[Z^j] \cong \sum_{l=1}^{m}\sum_{k=1}^{3} w_{l,k}(Z(l,k))^j \tag{A.4}$$

Then, central moments are calculated from raw moments using the general formula reported in (A.5).

$$\theta_j = \sum_{i=0}^{j}\binom{j}{i}(-1)^{j-i}\vartheta_i\vartheta_1^{j-i} \tag{A.5}$$

Finally, series expansions, such as Gram-Charlier, can be used to reconstruct the shape of the PDF of output Z starting from the knowledge of central moments.

B. Gram Charlier expansion

Gram-Charlier series of type A is here adopted [17]. The PDF of a generic random variable X is approximated with a PDF of the form $g(x)=d_n(x)\,\phi(x)$, where $\phi(x)$ is a normal PDF with zero mean and unit variance. The power series $d_n(x)$ is chosen so that $g(x)$ has the same first moments as the PDF of X, and it is approximated by using Hermite polynomials. In particular, using Hermite polynomials of order 3 and 4, the approximated PDF $g(x)$ is obtained as shown in (A.6). More details can be found in [17].

$$g(x) = \phi(x)\cdot\left\{1 + \frac{\gamma_1}{3!}He_3(x) + \frac{\gamma_2}{4!}He_4(x)\right\} \tag{A.6}$$

where γ_1 and γ_2 are respectively the skewness and the excess of kurtosis, i.e. kurtosis-3.